A study of the R.F.Q. Radial Matching Section

R. Duperrier

CEA/DSM/DAPNIA/SEA/IPHI 2000/09

February 19^{th}, 1999

Contents

Introduction

Since in R.F.Q. (Radio Frequency Quadrupole) local Twiss parameters depend on time or radio frequency phase, it is necessary to match the time dependant beam at the entrance of the main part of the R.F.Q. through a so called Radial Matching Section (R.M.S.). To get this matching in time, a ramp on focusing strength $F_{foc.}(z)$ is made over a distance of several unit cells $\beta\lambda/2$ in length. The first step when designing this section is to generate $F_{foc.}(z)$ in an analytical or numerical way. Analytically, the designer selects amoung series which are suitable to get the best matching and to give continuity of the electric potential at the interface between the R.M.S. and the rest of the R.F.Q.. Series are solutions of Laplace equation. This gives a vane profile at the entrance of the structure as described in figure 0.1.

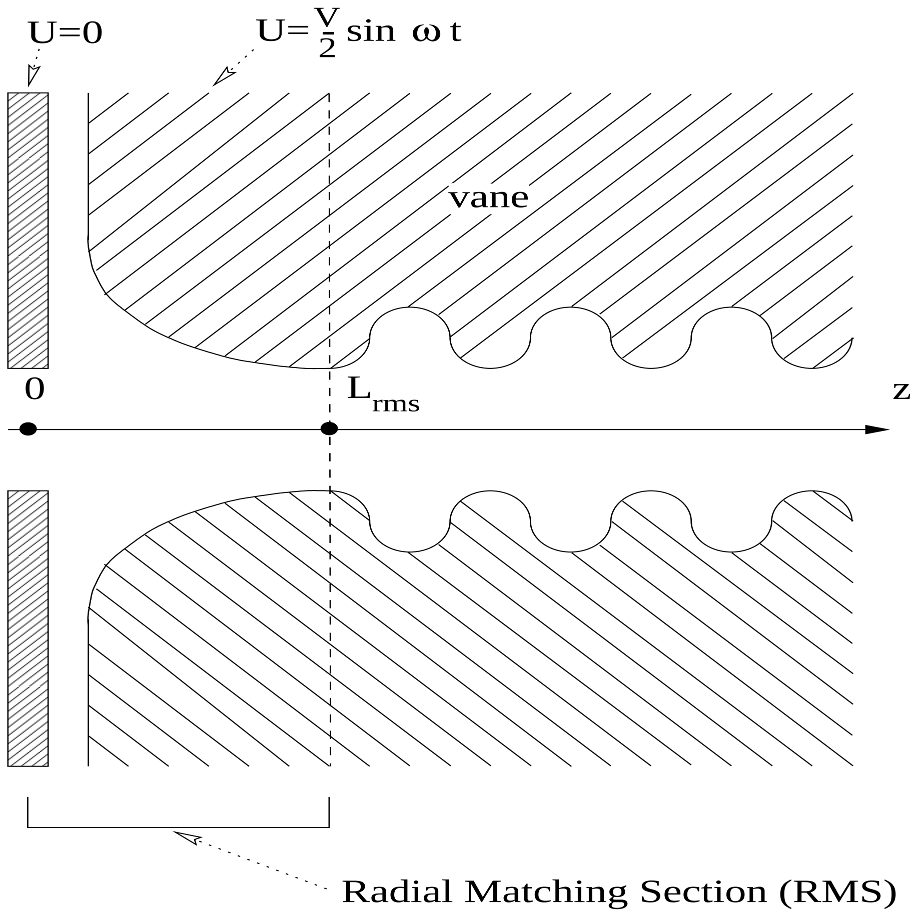

Figure 0.1: Longitudinal geometry of electrodes at R.F.Q. entrance.

Chapter 1

Method and formulations of the potential

1.1 Method used to optimize R.F.Q. entrance

Let us briefly recall the method used to optimize a matching section. The designer has first to find beam parameters that give good matching to a FD channel (Focusing Defocusing, see figure 1.1) which occupies R.F.Q. beginning. This channel is described with a very good accuracy by the following formula:

$$U(r,\theta,t) = \frac{V}{2}[A_{01}(\frac{r}{R_0})^2\cos(2\theta) + A_{03}(\frac{r}{R_0})^6\cos(6\theta)]\sin(\omega_{rf}t + \varphi_{rf}) \tag{1.1}$$

where R_0 is the vane aperture, V the inter-vane voltage, A_{01} and A_{03} respectively the quadrupolar and the duodecapolar coefficients. Those coefficients only depend on ρ/R_0 where ρ is the radius of curvature of the pole [1, 2]. When this first step is achieved, the designer makes the hypothesis that transport in this part of the structure is reversible. This means that emittance variations are small enough to be neglected. We will discuss this point in the chapter 3. Then the matched beam at the end of the RMS with different phase are transported to the entrance of the section with enveloppes code or mutli-particle code. Characteristics of the beam at the beginning of the section have to be very closed for each radio frequency phase. The $<\alpha>$ and $<\beta>$ (means in respect to different phases) are then supposed to be the time independant Twiss parameters that give the best matching for the R.F.Q.. In order to optimize this process, the beam is finally transported in the real direction through the R.M.S. and the FD channel. The effectiveness, $F_{mis.}$, of the radial matching section can be measured by the maximum value of the mismatch factor, $F_{mis.}(z,\varphi_{rf})$, in respect to z and phase in FD channel. At each step of calculation, $F_{mis.}(z,\varphi_{rf})$ is evaluated. $F_{mis.}(z,\varphi_{rf})$ is defined by the formula:

$$F_{mis.}(z,\varphi_{rf}) = \frac{\hat{X}_{mismatched}(z,\varphi_{rf})}{\hat{X}_{matched}(z,\varphi_{rf})} - 1 \tag{1.2}$$

where $\hat{X}_{matched}$ is the reference which has been calculated in the first step , $\hat{X}_{mismatched}$ is the new beam enveloppe size. Values of a few percent indicate a very effective matching section and any value less than 0.1 is probably acceptable. In the case where this value is estimated too high, the designer can change some parameters of the matching section like its length or coefficients in the series.

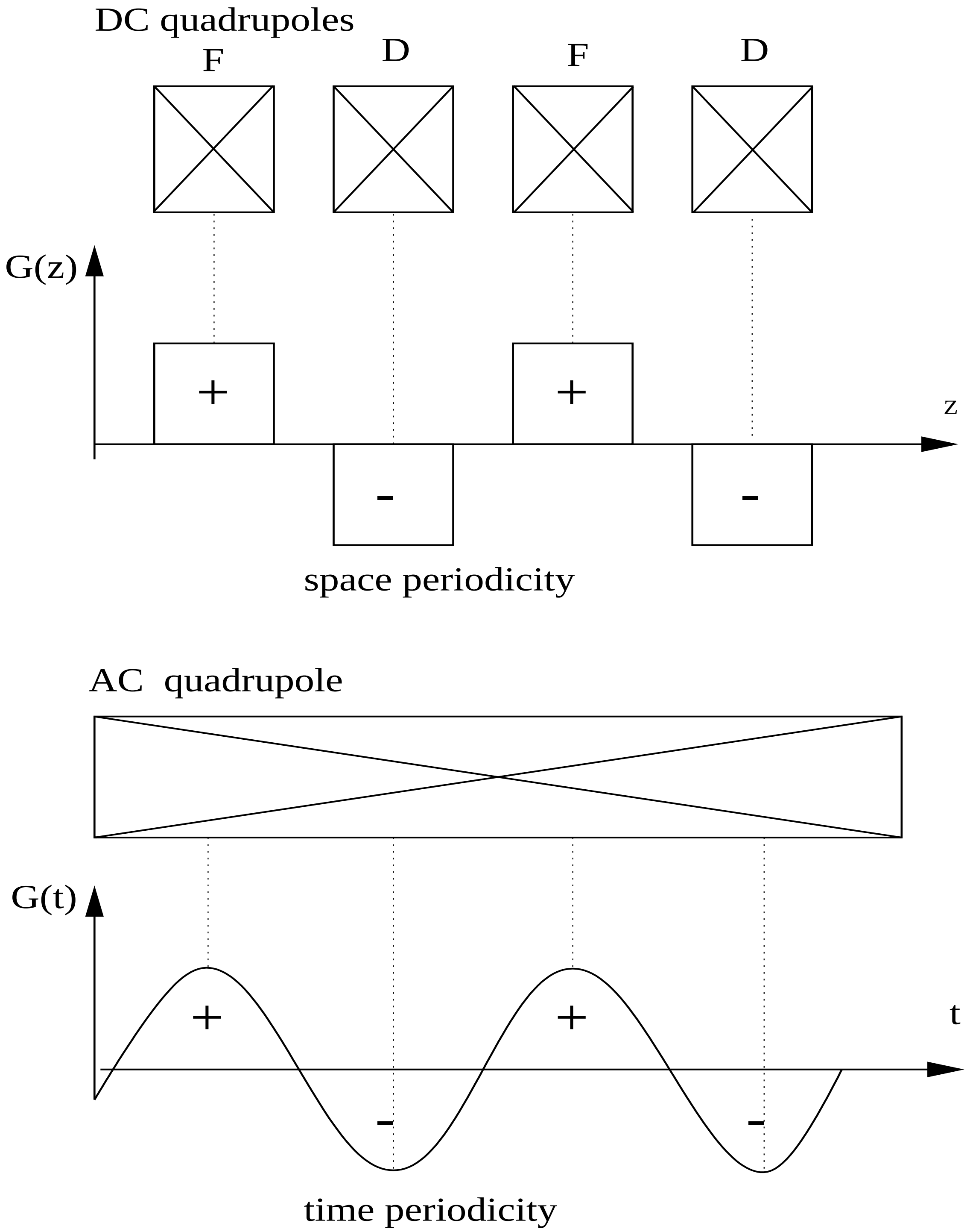

Figure 1.1: Alternating gradient focusing with 'space' and 'time' periodicity.

1.2 Main formulations for R.M.S.

Several forms have been used to describe the potential function in the radial matching section [3, 4, 5]. Note that [3] (F2) is the reference for PARMTEQM the most common code for dynamics of high current beam in R.F.Q.. In this study, we consider the following series:

$$\begin{aligned}
F1 : U(r,\theta,z) &= \frac{V}{2}\frac{z}{L_{rms}}\sum_{m=1,3}[A_{0m}(\frac{r}{R_0})^m\cos(m\theta)] \\
F2 : U(r,\theta,z) &= \frac{V}{2}\sum_{m=1,3}A_m[I_{2m}(kr)\sin(kz)+3^{-(2m+1)}I_{2m}(3kr)\sin(3kz)]\cos(2m\theta) \\
F3 : U(r,\theta,z) &= \frac{V}{2}\sum_{m=1,3}\sum_{n=0,N}[A_{0m}(\frac{r}{R_0})^{2n+m}\cos(m\theta)G_n(z)] \\
F4 : U(r,\theta,z) &= \frac{V}{2}A_1I_2(kr)\cos(2\theta)\sin(kz) \\
F5 : U(r,\theta,z) &= \frac{V}{2}\frac{z}{L_{rms}}A_{01}(\frac{r}{R_0})^2\cos(2\theta)
\end{aligned}$$

where:

$$G_n(z) = (-1)^n\frac{2!}{4^n n!(n+2)!}\frac{\partial^{2n}G_0(z)}{\partial z^{2n}} \qquad \text{with:} \qquad G_0(z) = \frac{\exp(-\alpha_q(\frac{z-L_{rms}}{L_{rms}})^{2m_q})-\exp(-\alpha_q(\frac{z+L_{rms}}{L_{rms}})^{2m_q})}{1-\exp(-2^{2m_q}\alpha_q)}$$

and:

$$k = \frac{\pi}{2L_{rms}}$$

For each formulation, the different sets of coefficients are chosen to get the best connexion with formula 1.1, except F4 which considers a connexion to a pure quadrupole. For F3, α_q, m_q and L_{rms} can be adjusted to get the best matching. For the other formulations, only the length of the section, L_{rms}, can be adjusted.

Let us note the advantages and disadvantages of each formulation:

- F1 gives the best continuity with transverse components of formula 1.1. In z direction, the connexion is less smooth than with a sinusoidal profile.

- F2 gives a good continuity with transverse components of the FD channel for first orders. It allows a longitudinal component which vanishes at interface R.M.S./R.F.Q..

- F3 is very similar to F2. It allows more flexibility in the expansion.

- F4 gives a smooth connexion in longitudinal but is very simplified in transverse.

- F5 allows us to estimate the importance of the duodecapolar component in respect to F1.

Chapter 2

Comparison between formulations

2.1 Comparison with enveloppes code

In this study, we shall consider the following parameters for the beam and the structure:

Distribution	K.V.
$\varepsilon_{tot.,norm.}$	1. π.mm.mrad
Current	100 mA
Particles	protons
Kinetic energy	95 keV
Frequency cavity	352 MHz
Voltage	101.4 kV
R_0	4.11 mm
ρ/R_0	0.89
A_{01}	0.9826
A_{03}	0.0197

For the first step, the matched Twiss parameters are calculated by least mean squared method. The transport of the beam is simulated by solving the following equations:

$$\left\{ \begin{array}{l} \hat{X}'' + \frac{4<xF_x>}{\gamma m(\beta c)^2 \hat{X}} - \frac{2K}{\hat{X}+\hat{Y}} - \frac{\varepsilon^2}{\hat{X}^3} = 0 \\ \hat{Y}'' + \frac{4<yF_y>}{\gamma m(\beta c)^2 \hat{Y}} - \frac{2K}{\hat{X}+\hat{Y}} - \frac{\varepsilon^2}{\hat{Y}^3} = 0 \end{array} \right. \tag{2.1}$$

with:

$$K = \frac{eI}{2\pi\varepsilon_0 m(\gamma\beta c)^3}$$

I is the current, e and m the charge and the mass of the particle, γ and β the relatistic factors of the beam, ε_0 the permittivity of vacuum, c the speed of light. ε is kept constant. The expression $< xF_x >$ means that the external strength is linearized over the distribution. In order to simplify the numerical integration of 2.1, the Bessel series are truncated (6^{th} order max.). Using datas $(z_i, \hat{X}_i)$, we minimize with respect to A and B the quantity:

$$\sum_i \{\hat{X}_i - [A + B\cos(\frac{2\pi z_i}{\beta\lambda_{rf}} + \varphi_{rf})]\}^2$$

according to the hypothesis that profile of the matched beam, $\hat{X}_{matched}$, is defined by $A + B\cos(\frac{2\pi z}{\beta\lambda_{rf}} + \varphi_{rf})$ (see appendix A). Convergence of this process is fast. With less than 5 iterations, the matched (A,B) are determined with good accuracy ($F_{mis.}$ <0.01). In the figure 2.1, we can see the result after 3 iterations.

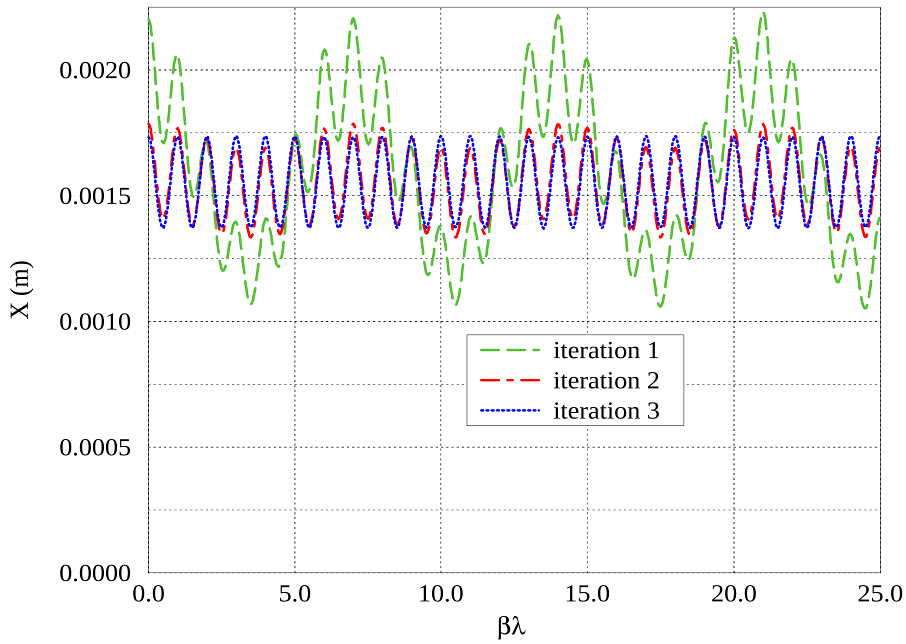

Figure 2.1: $\hat{X}(z)$ for the three first iterations of the minimization with respect to A and B.

Following the process described in 1.1, the mismatch factor as a function of the length of the R.M.S. obtained with different formulations is plotted in figure 2.2. Several comments about those results:

- figure 2.3 shows that a formulation, which does not take into account the duodecapolar component and the fact the quadrupolar component is not pure ($A_{01} \neq 1$), gives a disgraced effectiveness of the section.

- figure 2.4 shows that taking into account that $A_{01} \neq 1$ is not sufficient, the duodecapolar component has to be include in the expansion.

- in figure 2.5, in order to get a smooth connexion with the rest of the R.F.Q., $F_{foc.}(z)$ must follow a shape like described in figure 2.6 in respect to F1 which follows a linear profile in z.

- 6 cells are adequate to get suitable effectiveness (mismatch factor less than one percent cannot be measured easily). Choosing a longer section gives a bigger and more convergent beam at the entrance of the tank, that means that the solenoid has to be placed closer. Consequently the free space where can be inserted diagnostics is shorter (see figure 2.7).

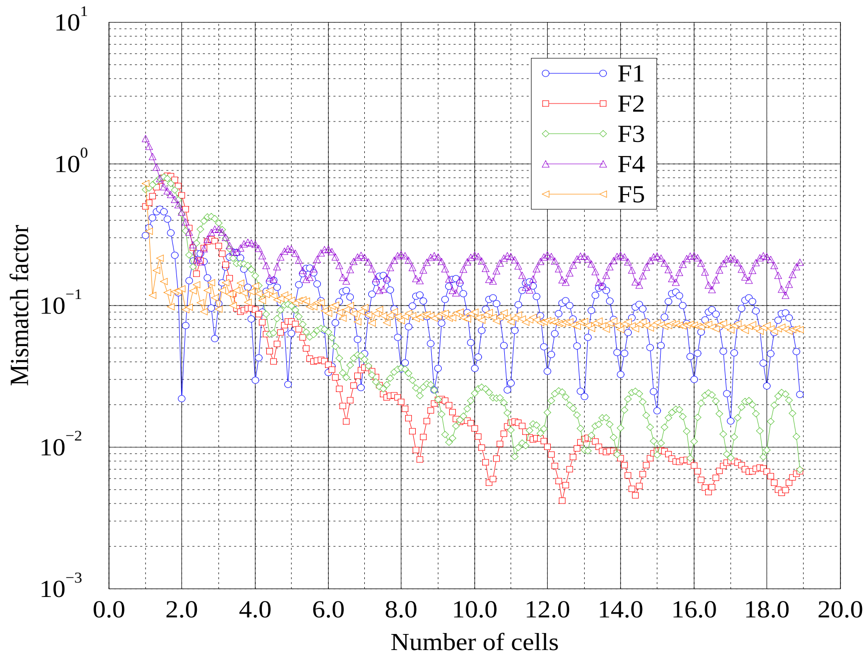

Figure 2.2: $F_{mis.}$ from 1 cell to 19 cells long for the different formulations (1 cell=$\beta\lambda/2$)

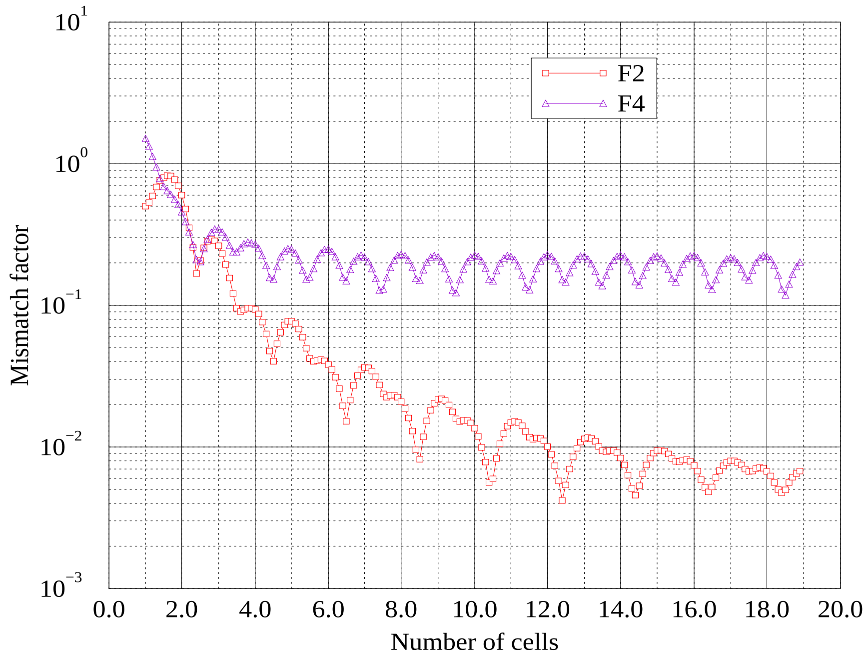

Figure 2.3: Results for F2 and F4

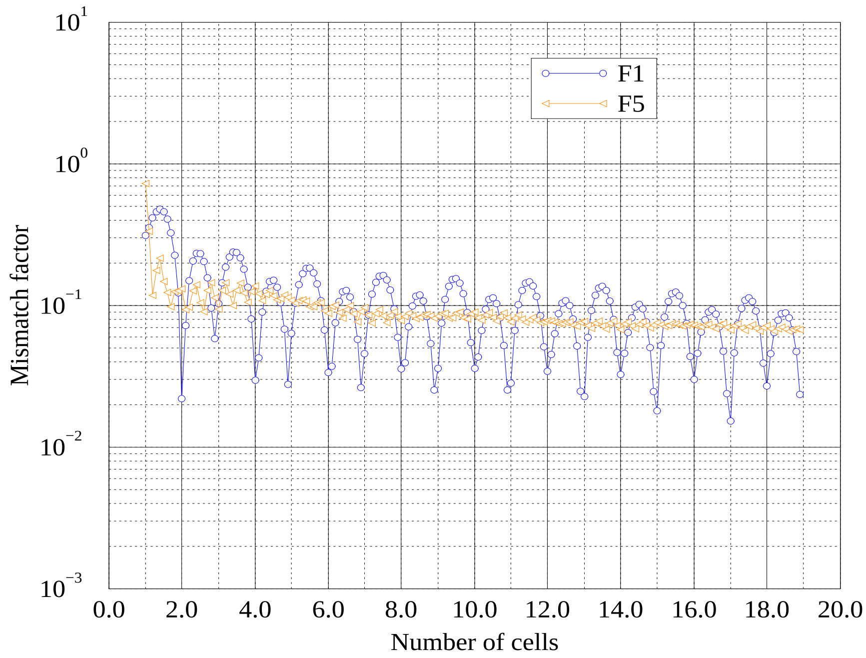

Figure 2.4: Results for F1 and F5

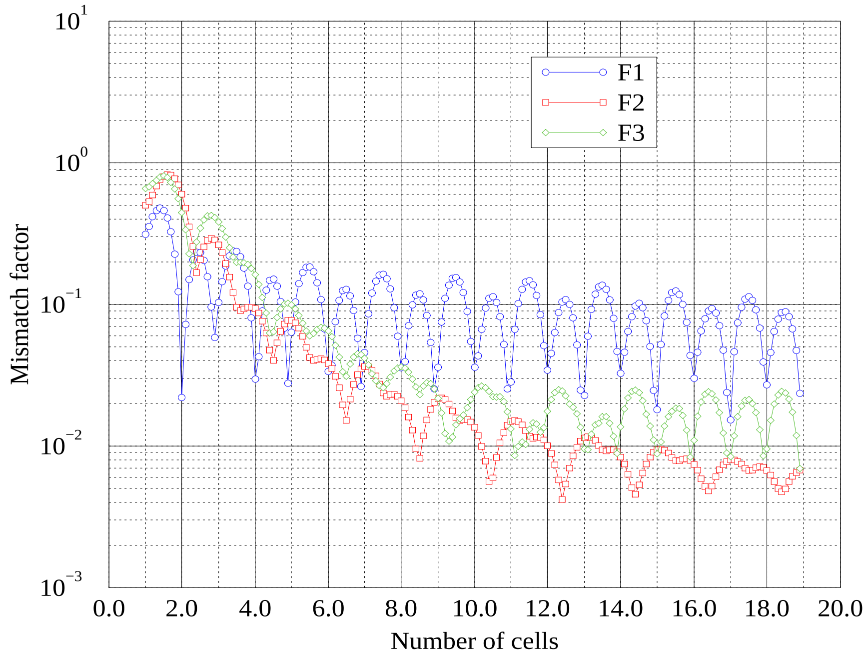

Figure 2.5: Results for F1, F2 and F3

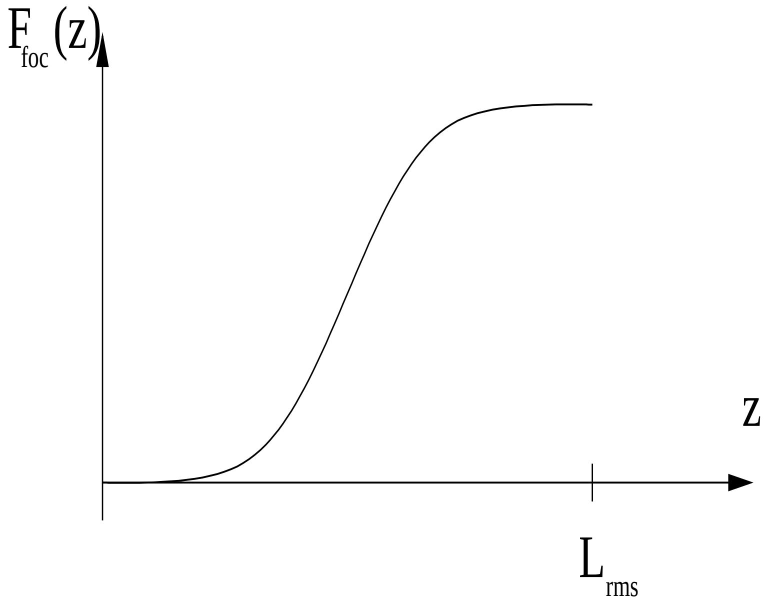

Figure 2.6: Suitable profile for $F_{foc.}(z)$

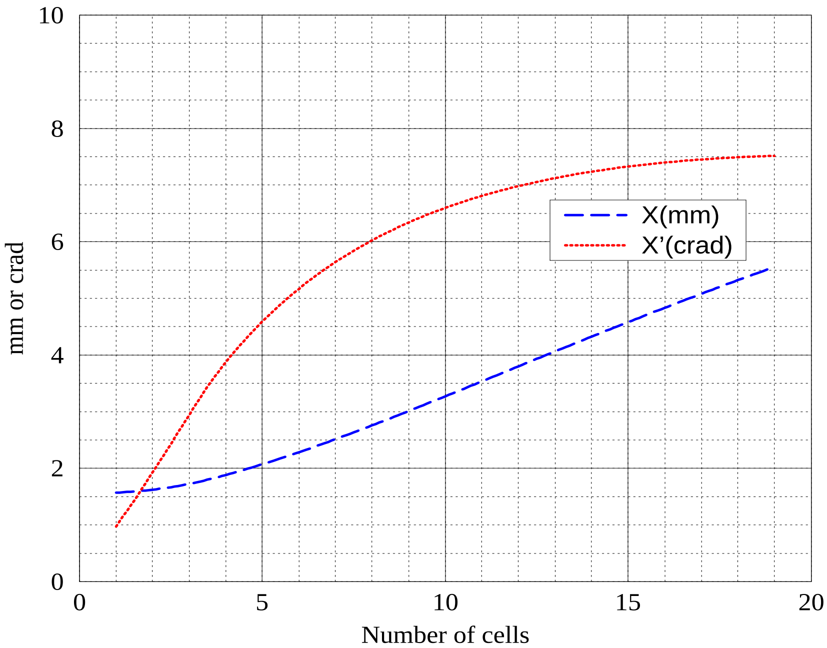

Figure 2.7: Beam size and convergence as a function of L_{rms} for F2 at R.F.Q. entrance.

2.2 Comparison with multi-particle code

In previous section, we have considered that ε kept constant during the run. This means that the variations of emittance due to space charge and mismatching in respect to the channel can be neglected. Following the same process with enveloppes code, we have calculated the mismatch factor from 1 to 19 cells long for the different formulations with a multi-particle code which allows emittance variations. The distribution is a 4-D waterbag with same root mean square (r.m.s.) parameters ($\varepsilon_{tot.,norm.}$ becomes 1.5 π.mm.mrad). As shown in figures 2.8, 2.9

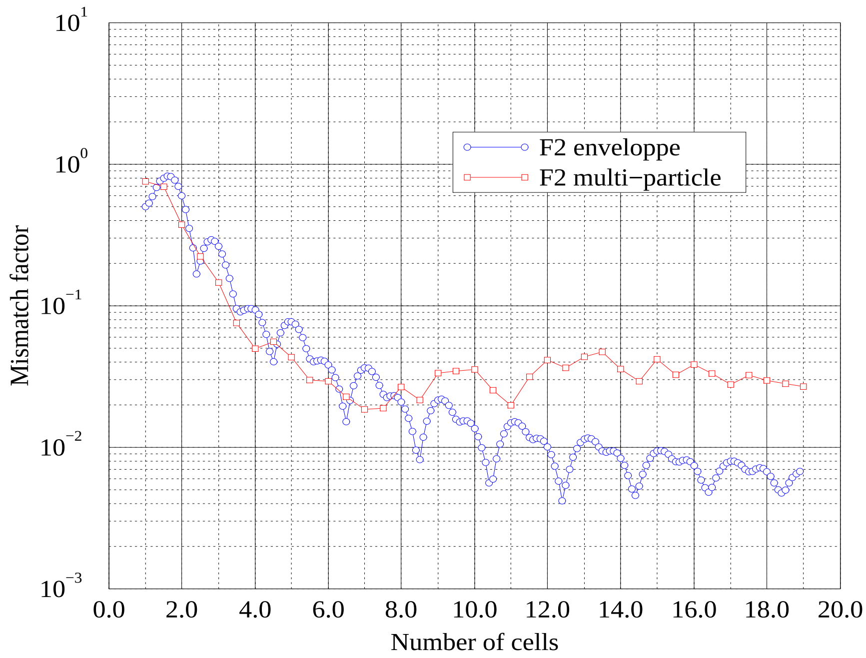

Figure 2.8: Results for F2 with enveloppe and multi-particle transport

and 2.10, the results are identical as much as effectiveness of the section is about $\sim$10 percent. It seems that emittance variations about a few percent can explain this result. Indeed, if we change the value of ε (5%) and simulate transport with enveloppe code, we get a mismatch of a few percent in respect to a few 0.1 percent before. In order to conclude, we estimate that a matching better than 1% requires to know the variations of ε during the run. However, it is not necessary to reach such accuracy with regard to the diagnostic performances and the masterchip of matching for the rest of the R.F.Q..

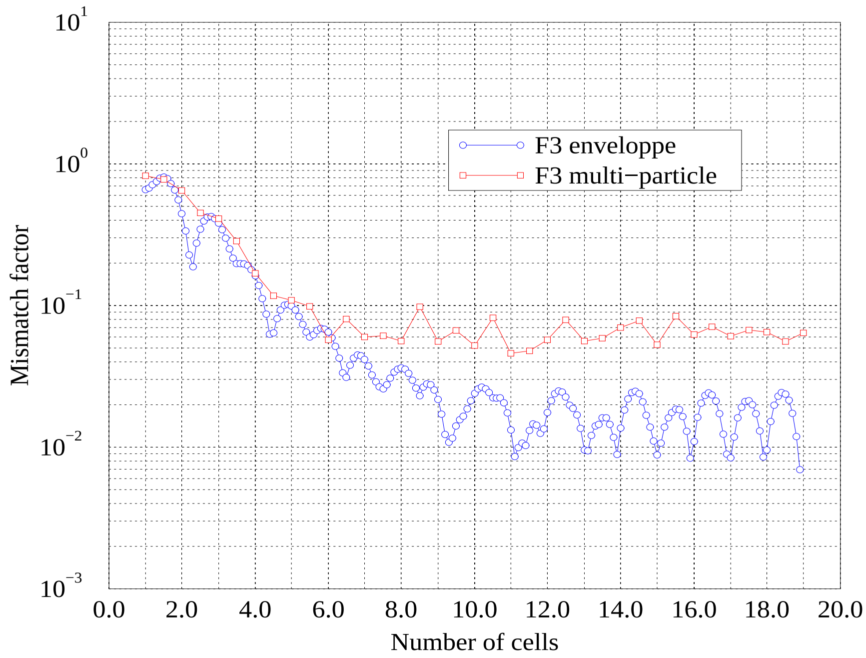

Figure 2.9: Results for F3 with enveloppe and multi-particle transport

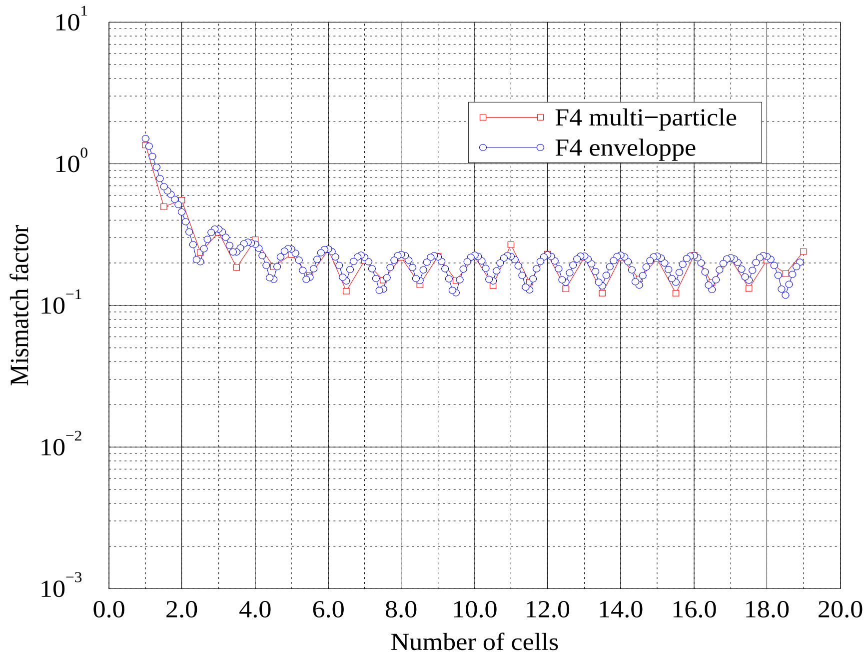

Figure 2.10: Results for F4 with enveloppe and multi-particle transport

Chapter 3

Limit of the method

The main hypothesis of the method is that the emittance's variations can be neglected. One may think that for high tune depression the transport could be not reversible [1]. Length of the section may play an additional part to this irreversibility. Longer the section is, higher emittance may grow (in order to reach equilibrium). To estimate a possible disgrace, we repeat the method for r.m.s. tune depression from 0.3 to 1., with 6, 12 and 18 cells R.M.S. long using F2. For each run, we calculate the difference between the mismatch factor obtained in the FD channel *before* the back and forth through the R.M.S. and the mismatch factor in the FD channel *after* the back and forth through the R.M.S. [2]:

$$\Delta \quad = \quad (F_{mis})_{After\ passage} - \ (F_{mis})_{Before\ passage} \tag{3.1}$$

As shown in figure 3.1, Δ variations may be omitted (a few percent) with regard to fixed tolerances ($F_{mis} < 5\%$ may be neglected). Note that is true also for high tune depression. As low as a mismatch factor of 10 percent is sufficient, we conclude that space charge does not induce an emittance growth such as irreversible transport occures[3].

[1] For the previous runs, the r.m.s. tune depression is 0.67.

[2] The tolerance for F_{mis} is fixed to 5%, any lower value may be neglected.

[3] For $\sigma/\sigma_0 = 0.3$, the emittance grows to 10 % in the R.M.S.

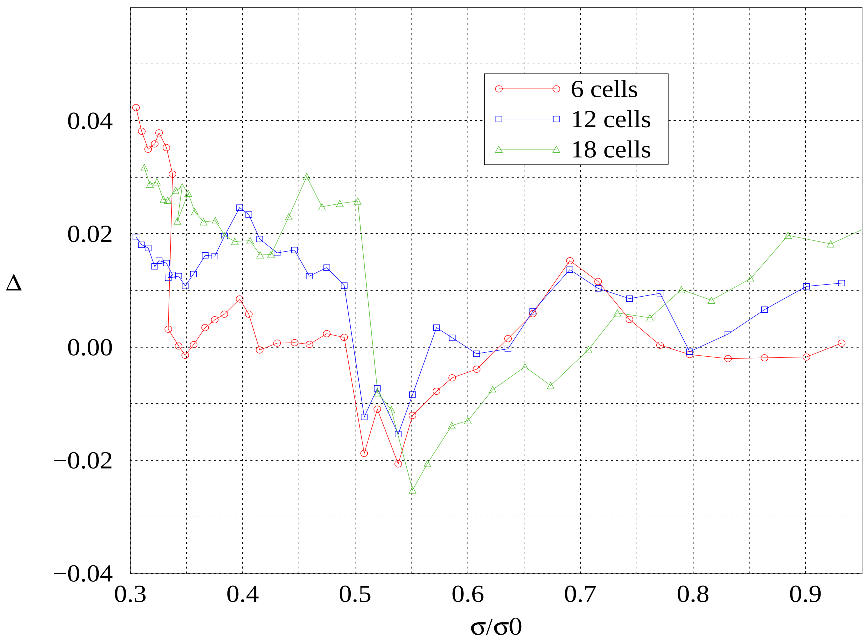

Figure 3.1: Δ from 0.3 to 0.95 r.m.s. tune depression for different L_{rms}

Conclusion

The method used in this paper to get the matched Twiss parameters for the R.F.Q. entrance is available for a large scale of r.m.s tune depression (from 0.3 to 1.). A 6 cells long section is an optimum choice with regard to reached matching and requirements for solenoid in the low energy line. Formulation used in PARMTEQM [3] gives the best performance but the other formulations are sufficient if we take into account the diagnostic performances. All these different points have lead to choose the following parameters for R.F.Q. of the IPHI project radial matching section: 6 cells long and the formulation F2.

Aknowledgment

I thank Jean-Michel Lagniel and Nicolas Pichoff for their comments and suggestions.

Bibliography

[1] K.R. Crandall, Effects of vane-tip geometry on the electric fields in Radio-Frequency Quadrupole linacs, L.A.N.L. report LA-9695-MS, 1983.

[2] R. Duperrier, Le potentiel électrique dans la zone utile d'un R.F.Q., C.E.A. report CEA/DSM/DAPNIA/SEA/9844, 1998.

[3] K.R. Crandall, R.F.Q. radial matching sections and fringe fields, the Linac Conference, 1981.

[4] J.L. Laclare & A. Ropert, The Saclay R.F.Q., C.E.A. report CEA/DSM/LNS/063, 1 june 1982.

[5] N. Tokuda & S. Yamada, New formulation of the R.F.Q. radial matching section, the Linac Conference, 1981.

Appendix A

Process to get the matched A and B:

We want that:

$$\frac{\partial}{\partial A}\sum_{i=1}^{N}\{\hat{X}_i - [A + BC(z_i)]\}^2 = 0$$

with:

$$C(z_i) = \cos(\frac{2\pi z_i}{\beta\lambda_{rf}} + \varphi_{rf})$$

then:

$$\begin{aligned}\sum_{i=1}^{N}\hat{X}_i &= \sum_{i=1}^{N} A + \sum_{i=1}^{N} BC(z_i)\\ &= NA + B\sum_{i=1}^{N} C(z_i)\end{aligned}$$

and:

$$\frac{\partial}{\partial B}\{\sum_{i=1}^{N}\{\hat{X}_i - [A + BC(z_i)]\}^2\} = 0$$

this gives:

$$\sum_{i=1}^{N}\hat{X}_i C(z_i) = A\sum_{i=1}^{N} C(z_i) + B\sum_{i=1}^{N} C(z_i)^2$$

we have to solve:

$$\begin{pmatrix} N & \sum_{i=1}^{N} C(z_i) \\ \sum_{i=1}^{N} C(z_i) & \sum_{i=1}^{N} C(z_i)^2 \end{pmatrix}\begin{pmatrix} A \\ B \end{pmatrix} = \begin{pmatrix} \sum_{i=1}^{N}\hat{X}_i \\ \sum_{i=1}^{N}\hat{X}_i C(z_i) \end{pmatrix}$$

finally:

$$\Longrightarrow \begin{pmatrix} A \\ B \end{pmatrix} = \frac{1}{\Delta}\begin{pmatrix} \sum_{i=1}^{N} C(z_i)^2 & -\sum_{i=1}^{N} C(z_i) \\ -\sum_{i=1}^{N} C(z_i) & N \end{pmatrix}\begin{pmatrix} \sum_{i=1}^{N}\hat{X}_i \\ \sum_{i=1}^{N}\hat{X}_i C(z_i) \end{pmatrix}$$

with:

$$\Delta = N\sum_{i=1}^{N} C(z_i)^2 - [\sum_{i=1}^{N} C(z_i)]^2$$

List of Figures